[Article ID] 1003- 6326(2002)01- 0006- 05

Crystal structure and thermal stability of martensite in Cu-24Al-3Mn alloy①

LI Zhou(李 周)[1,2], WANG Ming-pu(汪明朴)[1], CAO Ling-fei(曹玲飞)[1],
SU Yu-chang(苏玉长)[1], XU Gen-ying(徐根应)[2]
(1. Department of Materials Science and Engineering, Central South University, Changsha 410083, China;
2. Department of Materials Science and Engineering, Hefei University of Technology, Hefei 230009, China)

[Abstract] The crystal structure and thermal stability of the martensite in Cu-24Al-3Mn (mole fraction, %) alloy were studied by X-ray diffraction, electron diffraction, $V-t$ curve measurement. The 18R martensite with fairly perfect long-range order can be obtained by water-quenching the alloy. The atoms distribution on the basal plane of the martensite is as follows: Ⅰ, 3/25 Mn+ 22/25 Cu; Ⅱ, 3/25 Al+ 22/25 Cu; Ⅲ, 18/25 Al+ 7/25 Cu, correspondingly, the parent phase may have Heusler structure. From the electron diffraction result, the crystal structure is determined to be of a modified 18R type but closely approaching orthorhombic 18R type, its lattice parameters are determined to be a= 0.4474 nm, b= 0.5229 nm, c= 3.815 nm and β= 89.6° from the X-ray diffraction results. The obtained alloy has a higher thermal stability than that of the conventional Cu-Zn-Al alloy.

[Key words] shape memory alloy; Cu-Al-Mn alloy; martensite; crystal structure; thermal stability
[CLC number] TG146 [Document code] A

1 INTRODUCTION

Cu-based shape memory alloys (SMA) were studied by many authors in recent years[1~13]. It is convinced that the shape memory effect is associated with thermoelastic transformation from B_2 (or DO_3) to 9R (or 18R), 3R and 2H structure depending on the alloy composition, heat-treatment and the stress-induced condition. Many papers reported that the 9R (or 18R), 2H-type martensite possesses a monoclinic unit cell[3,5,6]. Another question in the Cu-based SMA is the martensite stabilization. It is an obvious phenomena that the monoclinic lattice of martensite transforms into the orthorhombic one when the martensite stabilization occurs. Thus the monoclinic angle can be considered to be an important lattice parameter to measure the degree of difficulty for the martensite stabilization. Before the martensite stabilization takes place, the monoclinic angle β is 90° (orthorhombic lattice) or is very near 90°, its lattice transformation from monoclinic one into orthorhombic one can be restraint and the martensite stabilization is uneasy to occur during aging in the martensite. Cu-24Al-3Mn (mole fraction, %) alloy being reported here is designed on the basis of this point.

2 EXPERIMENTAL

Cu-24Al-3Mn (mole fraction, %) alloy was induction melted, cast into flat ingots, homogenized at 1 123 K for 24 h, then hot-rolled into sheets of 1mm thick after the surface defects of the ingots were cut off. The sheets were solution-treated at 1 073 K for 10 min and then water-quenched. The transformation temperature determined by $\rho-T$ curve was M_s= 503 K (Fig. 4(a)). The specimen was mechanically polished to 0.15 mm, and then jet electro-polished in a solution of $\varphi(H_3OH)$: $\varphi(HNO_3)$ = 2: 1 at about 253 K. The electron microscope used is an H800 operated at 200 kV. X-ray diffraction experiment and data processing were performed on a D-5000 diffractometer with powder specimens which passed through 200 mesh sieve. The powder specimens were solution-treated at 1 073 K for 10 min in a sealed quartz tube filled with argon, followed by water-quenching.

3 RESULTS AND DISCUSSION

3.1 X-ray diffraction of martensite

Fig. 1 shows the X-ray diffraction profile of the martensite in the tested alloy at room temperature. It can be seen that the diffraction peaks labeled by numbers 5, 7, 8, 10~ 14 seem to be independent ones respectively. This diffraction pattern is obviously different from that of Cu30Au26Zn45 (mole fraction, %) (M18R, β= 87.5°)[8], Cu-18Zn-14Al (mole fraction, %) (M18R, β= 88.6°)[11] and Cu-40Zn (mole fraction, %) (M9R, β= 88.43°)[3]. WANG, one

① [Foundation item] Project (50071069) supported by the National Natural Science Foundation of China
[Received date] 2001- 03- 01; [Accepted date] 2001- 06- 08

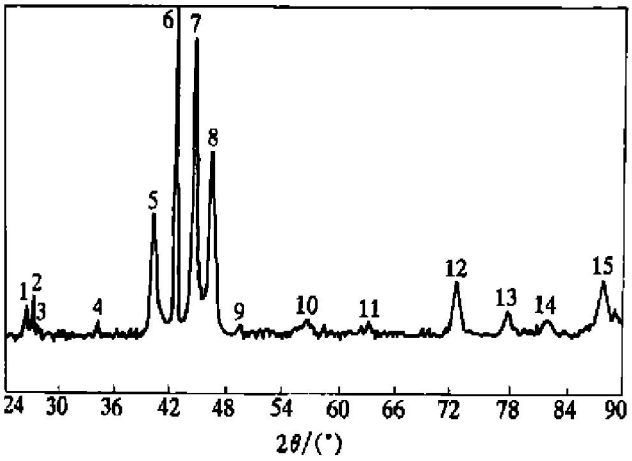

Fig. 1 X-ray diffraction spectrum of water-quenched martensite of Cu-24Al-3Mn alloy

of the authors of this paper studied the stabilization process of martensite in Cu-13Zn-15Al (mole fraction, %)[13]. With the increase of the aging temperature in the martensite state, the diffraction pairs of the martensite in Cu-15Al-13Zn, such as $(12L)$, $(20\bar{L})$ and $(04L)$, $(32\bar{L})$ tended to get closer, and $\beta \rightarrow 90°$. The diffraction pattern of quenched martensite in the tested alloy is similar to that of the stabilized martensite as mentioned above. So we may draw the initial judgment that the martensite in the tested alloy maybe possess the N18R structure and the martensite stabilization is uneasy to occur. But the structure of martensite tested can not be indexed to be N18R type actually because there exists a deviation between calculated d_{cal1}-value (d_{cal1}) and observed d_{obs1}-value (d_{obs1}) (listed in Table 1) in the same diffraction, such as $(12L)$ and $(20\bar{L})$, $(04L)$ and $(32\bar{L})$, and the greatest one is up to 0.01 nm which goes beyond the experimental error range.

By carefully measuring the R-value of the electron diffraction spots in Figs. 2(b) ~ (e), we find that all of the R-value of the $(12L)$ and $(20\bar{L})$ diffraction spots have fine difference. So the X-ray diffraction peaks mentioned above are not really independent ones. It is necessary to separate these diffraction peaks. Each of the measured d_{obs2}-value and relative intensity of diffraction peaks are obtained after the diffraction peaks were separated and are listed in the fifth and seventh column in Table 1. The lattice parameters determined by the d_{obs2}-value (d_{obs2}) are $a = 0.4475$ nm, $b = 0.5229$ nm, $c = 3.815$ nm, $\beta = 89.6°$. Using these lattice parameters, the calculated d_{cal2}-value can be obtained which are listed in the sixth column in Table 1. It can be seen that the d_{cal2}-values (d_{cal2}) coincide perfectly with the d_{obs2}-values. Therefore it can be concluded that the structure of martensite in the tested alloy is still M18R type but it is very close to orthorhombic structure (N18R).

Fig. 3 shows the hard sphere atomic structure model of the M18R martensite[6]. There are only 4

Table 1 X-ray diffraction data measured and that calculated of water-quenched martensite of Cu-24Al-3Mn alloy

Peak No.	HKL	d_{obs1}/ nm	d_{cal1}/ nm	d_{obs2}/ nm	d_{cal2}/ nm	$(I/I_{12\bar{8}})_{obs} \times 10^{-2}$	$(I/I_{12\bar{8}})_{cal} \times 10^{-2}$
1	111	0.3388	0.3388	0.3388	0.3388	6.8	6.7
2	019	0.3286	0.3286	0.3286	0.3286	8.6	8.8
3	$10\bar{8}$	0.3257	0.3260	0.3257	0.3260	1.7	1.7
4	020	0.2606	0.2598	0.2606	0.2609	1.3	1.6
5	$12\bar{2}$ 202	0.2237	0.2183	0.2240 0.2221	0.2241 0.2220	25.5 25.2	25.5 23.6
6	0018	0.2119	0.2119	0.2119	0.2119	78.5	78.0
7	$12\bar{8}$ 208	0.2027	0.2105	0.2031 0.2026	0.2033 0.2028	100.0 42.4	100.0 43.9
8	1210 $20\bar{1}0$	0.1949	0.1839	0.1953 0.1893	0.1949 0.1895	86.5 35.6	87.4 38.4
9	2014	0.1799	0.1797	0.1799	0.1797	4.6	4.3
10	1216 $20\bar{1}\bar{6}$	0.1619	0.1627	0.1657 0.1618	0.1660 0.1621	8.8 9.7	9.1 10.1
11	2020 $12\bar{2}\bar{0}$	0.1468	0.1462	0.1466 0.1460	0.1463 0.1458	1.4 3.2	1.7 3.7
12	040 320	0.1300	0.1276	0.1317 0.1296	0.1316 0.1295	13.0 23.4	13.3 24.7
13	2026 $12\bar{2}\bar{6}$	0.1228	0.1223	0.1226 1.222	0.1226 1.221	4.9 15.6	5.7 16.8
14	1228 $20\bar{2}\bar{8}$	0.1172	0.1169	0.1175 0.1160	0.1178 0.1161	13.6 5.1	15.2 5.2
15	3218 $32\bar{1}\bar{8}$	0.1196	0.1104	0.1108 0.1095	0.1108 0.1103	13.6 14.2	14.7 15.0

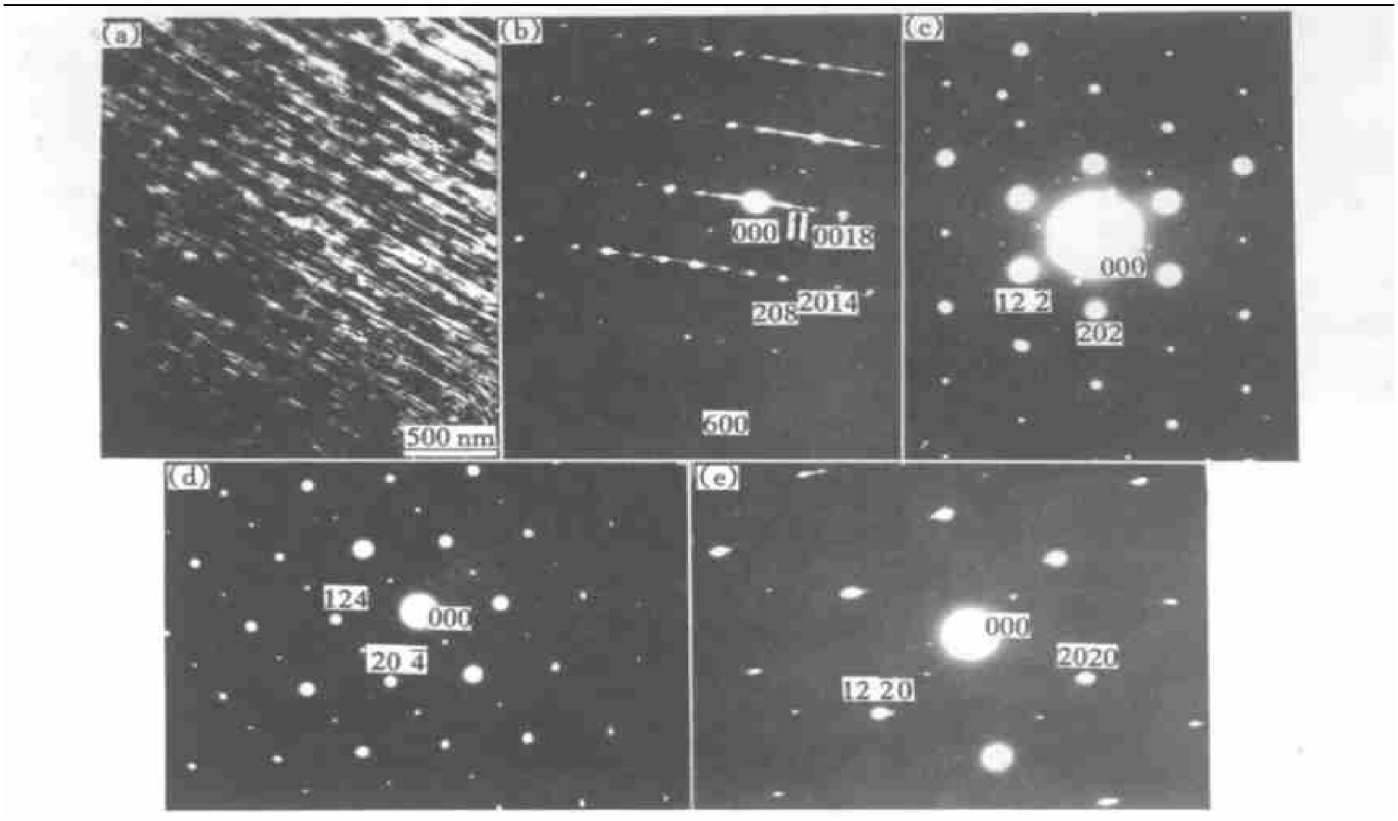

Fig. 2 Micrograph (a) and diffraction patterns (b) ~ (e) with zone axis $[0\ \bar{1}0]$, $[\ 2\ \bar{3}\ \bar{2}]$, $[\bar{2}3\ \bar{1}]$ and $[10\ \bar{1}5\ \bar{1}]$ respectively for M18R

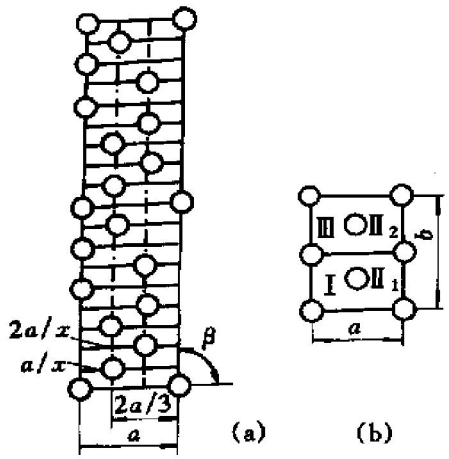

Fig. 3 Crystal structure model of M18R martensite

kinds of different positions, i.e., I, II_1, II_2, III on the basic plane (Fig. 3(b)). No matter how many sorts and great amount of atom are distributed, its structure factor can be expressed as

$$F_{HKL} = F_a \cdot F_1 \cdot F_2 \cdot F_3 = \{ f_{\mathrm{I}} + f_{\mathrm{II}} \exp 2\pi i (K/2) + f_{\mathrm{II}1} \exp 2\pi i (H/2 + K/4) + f_{\mathrm{II}2} \exp 2\pi i (H/2 + 3K/4) \} \cdot \{ 1 + \exp 2\pi i \cdot (H/x + K/2 + L/18) + \exp 2\pi i (2H/x + 2L/18) \} \cdot \{ 1 + \exp 2\pi i (H/3 + K/2 + 3L/18) + \exp 2\pi i \cdot (2H/3 + 6L/18) \} \cdot \{ 1 + \exp 2\pi i (K/2 + L/2) \}$$

where $x = a/x'$, $x' = \cos\beta/9 + a/3$, the F_a is the structure factor of the basic plane.

Considering the difference of the scattering factor between every two kinds of the atoms for Cu, Al and Mn and the X-ray diffraction data, the rational atom distribution on basal plane is that the atom on position I is 3/25Mn + 22/25Cu, II is 3/25Al + 22/25Cu, III is 18/25Al + 7/25Cu.

Then the structure factor of the basic plane can be expressed as follows:

For the fundamental diffraction, $F_a = 73/25 f_{Cu} + 24/25 f_{Al} + 3/25 f_{Mn}$;

For the *nn* (the ordering state of I and II, III and II) order diffraction, $F_a = 12/25 f_{Al} + 3/25 f_{Mn} - 15/25 f_{Cu}$;

For the *nnn* (the ordering state of I and III) order diffraction, $F_a = 3/25 f_{Mn} + 15/25 f_{Cu} - 18/25 f_{Al}$.

With the lattice parameters obtained from the experiment, $x = 2.94$ can be extracted. Using the formula F_{HKL} and considering the Lorentz-polarization and multiplicity factors, the relative diffraction intensities of the diffraction peaks concerned can be calculated and shown in the eighth column of Table 1. It can be seen that the I_{cal} coincides with the I_{obs} satisfactorily.

3.2 Electron diffraction result

Information about the structure can be acquired from Fig. 2 as follows:

1) The distance between the strong reflection, that is, the reciprocal unit interlayer spacing (RUIS), is divided into three parts by two weaker reflection. This suggests that the crystal structure is a

kind of LPSO structure. These characteristics of the fundamental electron diffraction patterns are quite similar to those martensite of the 18R type structure found in the Cu-Au26-Zn45[6]. Sub-structures of the martensite are mainly the basal-stacking fault (Fig. 2(a)). The electron diffraction illuminates that all of the diffraction patterns can be indexed as that of 18R. A part of the typical electron diffraction patterns are shown in Fig. 2(b) ~ (e). Weak diffraction spot which is seen in the middle of the RUIS along the c^* axis (indicated by arrow "↓" in Fig. 2(b)) shows that the 18R martensite includes 2H structure, which may come from stacking fault of 18R basal-plane[7].

2) The angle between c^* axis and a^* axis is 90.4 ℃ (and so a axis and b axis is 89.6 ℃, Fig. 2(b)), which coincides with the result of X-ray diffraction. The d-value analyzing indicates that the interplanar spacing of $(12L)$ and $(20\bar{L})$, $(32\bar{L})$ and $(04L)$ are equal in N18R structure, but they are not equal in the M18R structure. The difference Δd between them increases with the decrease of the monoclinic angle β. A careful inspecting of the R-value of diffraction spots of $(12\bar{2})$ and (202) (Fig. 2(c)), (124) and $(20\bar{4})$ (Fig. 2(d)), (2020) and $(12\bar{2}\bar{0})$ (Fig. 2(e)), we discovered that the former ones are all shorter than the latter ones. Therefore the structure of martensite tested is still M18R structure.

3) According to the structure indicated in Fig. 2(b), changing the monoclinic angle β, we studied the electron diffraction intensity distribution on the rows of reflection spots lined up parallel to the c^* axis. The calculated and observed intensity of the (202), (208) and (2014) diffraction spots are listed in Table 2. It can be found that with the increase of angle β, the intensity of (202) diffraction spots decreases, that of the (208) diffraction spot increases, but that of (2014) diffraction spot changes little. The intensity distribution order of (202), (208) and (2014) diffraction spots is SMW when the monoclinic angle β is less than 88.5°. When the β is greater than 89°, the intensity order of (202), (208) and (2014) diffraction spots are MSW, which coincides with the experimental result (Fig. 2(b)). It indicates that the martensite in the tested alloy is M18R structure although the monoclinic angle β is so great as to closely approaching the N18R structure.

3.3 Hard atom structure model of M18R martensite

The lattice parameter of b-axis can be calculated (b_{cal}) by the atomic radii of Cu, Al, Mn atoms which are 0.128 nm, 0.134 nm, 0.143 nm respectively[6], and by the close contact hard sphere atom structure model, b_{cal} is 0.5350 nm ($> b_{obs}$ = 0.5229 nm). This illuminates that the atoms closely pack along the b-axis. The calculated b-value among [210] orientation ($b_{[210]cal}$), which is 0.5250 nm, is longer than the observed one ($b_{[210]obs}$), which is 0.5183 nm, illuminating that the atom closely pack along [210] orientation too. $b_{[210]obs}/b_{[210]cal}$ = 98.8%, which illuminates that the atom coordination number is between 8 to 12 by Goldschmidt theory. When the atom coordination number is less than 12, the atomic radii will constrict. Considering the constriction, the calculated lattice parameter coincides satisfactorily with the observed one. It means that the atomic distribution on the basic plane obtained by the outcome of X-ray diffraction is reasonable. Because the tested alloy is composed of Cu, Al, Mn, so the atomic radii of different elements are not of the same size. If the basal plane consisted of atoms of same size, it would form an exactly hexagon and the stacking positions along the a-axis of 1st and 2nd layers would be just $a/3$ and $2a/3$, respectively. On the other hand, when the basal plane consists of atoms of different sizes, arranging themselves in an order as mentioned above, unless the non-close packed structure in basal plane was obtained, the hexagon may be distorted, consequently, the stacking positions should be shifted from the $a/3$ and $2a/3$, which leads to a result that the monoclinic angle deviates from 90°. Therefore, it is difficult for the constituent atoms in the basic plane to form an exact hexagon because of the difference size of the constituent atoms and an ordered arrangement of martensite in the tested alloy, but the M18R structure with monoclinic angle β closely approaches 90° can be obtained.

3.4 Thermal stability of Cu-24Al-3Mn

Fig. 4(a) shows the $V-t$ curve of the tested al-

Table 2 Calculated and observed relative intensities, in comparing with those of normal 18R type structure (N18R) ($\times 10^{-2}$)

HKL	M18R (β= 87.5°)	M18R (β= 87.5°)	M18R (β= 88.5°)	M18R (β= 89.0°)	M18R (β= 89.6°)	N18R (β= 90.0°)	Observed
202	100.0	100.0	100.0	84.5	53.8	39.2	Middle (M)
208	39.9	57.4	82.3	100.0	100.0	100.0	Strong (S)
2014	8.6	10.5	12.6	12.7	9.7	7.9	Weak (W)

loy which was subjected to water-quenching treatment after solution treated at 800 ℃. Compared with the experimental result of Cu-13Zn-15Al (mole fraction, %) alloy shown in Fig. 4(b), we find that stabilization and decomposition take place in the Cu-13Zn-15Al (mole fraction, %) martensite during heat treatment after water-quenching at 800 ℃, and the thermoelastic martensite transformation does not take place after cooling. The results in detail for Cu-13Zn-15Al (mole fraction, %) alloy was published in Ref. [13]. For Cu-24Al-3Mn alloy, although the martensite stabilization takes place, the reverse thermoelastic transformation still takes place between 400 ℃ and 430 ℃, and the forward thermoelastic transformation takes place after cooling. The forward-reverse martensite transformation in the tested alloy stably takes place between 180 ℃ and 250 ℃ undergoing one thermal cycling. The thermoelastic martensite stabilization no longer occurs. The result mentioned above illuminates that the tested alloy has a high thermal stability. At 430 ℃, when the first reverse transformation finishes, the parent phase does not decompose yet. Except the first reverse transformation, the forward-reverse thermoelastic transformation stably takes place between 180 ℃ and 250 ℃ and the martensite stabilization is uneasy to occur in the following transformation cycling.

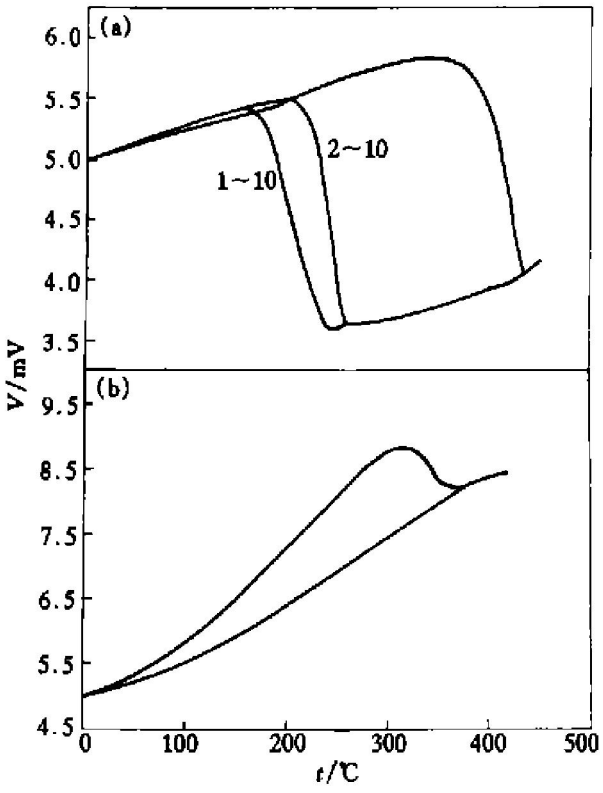

Fig. 4 V —t curve of transforming alloys
(a) —Cu-24Al-3Mn (mole fraction, %);
(b) —Cu-13Zn-15Al (mole fraction, %)

4 CONCLUSIONS

1) The martensite structure in the Cu-24Al-3Mn (mole fraction, %) alloy is determined to be of a modified M18R type, it closely approaches the N18R structure, and its lattice parameters are a = 0.4475 nm, b = 0.5229 nm, c = 3.815 nm and β = 89.6°. The atom distribution on the basal plane of martensite is as follows: Ⅰ, 3/25 Mn+ 22/25 Cu; Ⅱ, 3/25 Al+ 22/25 Cu; Ⅲ, 18/25 Al + 7/25 Cu.

2) The substructure of the martensite in Cu-24Al-3Mn (mole fraction, %) alloy is mainly basal stacking faults.

3) The Cu-24Al-3Mn alloy has a higher thermal stability than that of the convention Cu-Zn-Al alloy.

[REFERENCES]

[1] Saburi T, Wayman C M. Crystallographic similarities in shape memory martensites [J]. Acta Metallurgica, 1979, 27: 979- 995.

[2] Sade M, Lovey F C. The structure of the modified 2H martensite in Cu-Zn-Al [J]. Scripta Met, 1983, 17: 333 - 338.

[3] Tadaki T, Tokoro M, Shimizu K. Thermoelastic nature and crystal structure of the Cu-Zn martensite related to the shape memory [J]. Trans, JIM, 1975, 16: 285- 296.

[4] Lovey F C, van Tendeloo G, van Landuyt J, et al. The high resolution electron microscopy of twin interfaces in 2H and 18R martensites of Cu-Al alloys [J]. Scripta Met, 1985, 19: 1223- 1228.

[5] Saburi T, Nenno S, Kato S, et al. Configurations of martensite variants in Cu-Zn-Ga [J]. Journal of the Less Common Metals, 1976, 50: 223- 236.

[6] Kubo H, Shimizu K. Crystal structure of $Cu_{30}Au_{25}Zn_{45}$ martensite [J]. Trans, JIM, 1976, 17: 330- 338.

[7] Adachi K, Perkins J. Lattice image studies on the inter-variant boundary structure and substructure of Cu-Zn-Al 18R martensite [J]. Met Trans, 1985, 16A: 1551- 1566.

[8] Tadaki T, Okazaki H, Nakata Y, et al. Atomic configuration studied by ALCHEMI and X-ray diffraction of a stabilized M18R martensite in a β phase Cu-Au-Zn alloy [J]. Trans, JIM, 1990, 31: 941- 947.

[9] Pons J, Portier R. Accommodation of γ-phase precipitates in Cu-Zn-Al shape memory alloys studied by high resolution electron microscopy [J]. Acta Mater, 1997, 45(5): 2109- 2120.

[10] Tan J, Liu T F. As-quenched microstructures of Cu-14.2Al-xNi alloys [J]. Scripta Mater, 2000, 43: 1083 - 1088.

[11] WANG Ming-pu, JIN Zhan-peng, YIN Zhi-min. Order state and stability of martensite in an air-quenched Cu-Zn-Al [J]. Trans Nonferrous Met Soc China, 1996, 6 (3): 113- 118.

[12] WANG Ming-pu, LIU Jin-wen. On the stabilization of thermoelastic martensite in a Cu-Zn-Al alloy [J]. Acta Metall Sinica, 1990, 3A(6): 439- 441.

[13] WANG Ming-pu, WANG Shi-wei, JIN Zhan-peng. Relief phenomenon of stabilized martensites in a Cu-Zn-Al alloy [J]. J Cent South Univ Technol, (in Chinese), 1997, 28(1): 53- 56.

(Edited by HUANG Jin-song)